Available online at www.sciencedirect.com
ScienceDirect
Journal of Sound and Vibration 311 (2008) 9–19
JOURNAL OF SOUND AND VIBRATION
www.elsevier.com/locate/jsvi

Free vibration of composite skewed cylindrical shell panel by finite element method

Salil Haldar

Department of Applied Mechanics, Bengal Engineering and Science University, P.O.-B. Garden, Howrah 711103, India

Received 22 November 2006; received in revised form 7 August 2007; accepted 10 August 2007
Available online 11 January 2008

Abstract

In this paper a composite triangular shallow shell element has been used for free vibration analysis of laminated composite skewed cylindrical shell panels. In the present element first-order shear deformation theory has been incorporated by taking transverse displacement and bending rotations as independent field variables. The interpolation function used to approximate transverse displacement is one order higher than for bending rotations. This has made the element free from locking in shear. Two types of mass lumping schemes have been recommended. In one of the mass lumping scheme the effect of rotary inertia has been incorporated in the element formulations. Free vibration of skewed composite cylindrical shell panels having different thickness to radius ratios ($h/R = 0.01$–0.2), length to radius ratios (L/R), number of layers and fiber orientation angles have been analyzed following the shallow shell method. The results for few examples obtained in the present analysis have compared with the published results. Some new results of composite skewed cylindrical shell panels have been presented which are expected to be useful to future research in this direction.

1. Introduction

The cylindrical shell panels play an important role in modern engineering. Thus it is not surprising that a considerable number of literatures have been devoted to the study of the static and dynamic behavior of such structures.

Over 100 years ago Love developed two-dimensional theory of thin shells. In the last three decades, the developed refined two-dimensional theories of thin shells include important contribution of Sanders [1], Flugge [2] and Niordson [3]. Though, in these refined shell theories, the radial stress effect is neglected. The refined theories by Sanders [1], Flugge [2] and Niordson [3] provide very good results for the analysis of thin shells.

Initially, relative to the theory of thin shells, the theory of thick shells has received limited attention by the researchers. With the increase utilizations of thick shells and fiber-reinforced laminated composite shell structures in various engineering applications, it is important to develop a simple and accurate theory for thick shells. In thick shell particularly laminated composite shells, the transverse shear deformation may no longer be neglected.

E-mail address: salilhaldar@lycos.com

0022-460X/$ - see front matter © 2007 Elsevier Ltd. All rights reserved.
doi:10.1016/j.jsv.2007.08.022

Nomenclature

a	length of the square shell panel
E	modulus of elasticity of isotropic shell material
E_1	modulus of elasticity of composite material along fiber direction
E_2	modulus of elasticity of composite material perpendicular to fiber direction
G	modulus of rigidity
h	thickness of the shell panel
L	length of the shell panel
R	radius of the middle surface of the shell panel
α	skew angle of the shell panel
λ	dimensionless frequency parameter
v	Poisson's ratio
θ	subtended angle of the cylindrical shell panel
ρ	mass density of the shell material
ω	circular frequency in rad/s

Qatu [4,5], in his papers has presented the free vibration behavior of isotropic and composite shell panels. Dynamic and static analysis of open cylindrical shell freely supported along curved edges and having different boundary conditions along straight edges has been analyzed by Selmane and Lakis [6]. Lee and Han [7] have discussed the free vibration analysis of isotropic plates and shells using a nine-node degenerated shell element. In this analysis first-order shear deformation theory has been used. Liu et al. [8] have implemented the element free Galerkin method for static and free vibration analysis of general shell structures. The formulation has been verified through numerical example of static and vibration of spatial shell structures. A refined theory for thick spherical shell has been presented by Voyiadjis and Woelke [9]. The equations given in this paper do not only incorporate the effects of transverse shear deformation but also account for initial curvature as well as the radial stress. Hossain et al. [10] have presented an improved finite element model for the linear analysis of anisotropic and laminated doubly curved, moderately thick composite shell panels. The model has been developed considering first-order shear deformation theory. Both shallow and deep shells have been investigated. Kandasamy and Singh [11] have presented a numerical investigation of free vibration of skewed open cylindrical isotropic shells. In the formulation, first-order shear deformation theory and rotary inertia have been included. Thin and moderately thick shells have been studied.

In the present work, free vibration of laminated composite skewed cylindrical shell panels has been studied using the concept of shallow shell method. First-order shear deformation theory has been included in the present finite element formulation. The effect of rotary inertia has been included in the formulation.

2. Finite element formulation

The formulation is based on shallow shell theory. A typical shell element shown in Fig. 1 has been projected in the base plane. The location of the nodes 3, 7 and 11 are at the midpoint of the corresponding sides while nodes 2, 4, 6, 8, 10 and 12 are located at a distance of one third of the length of the corresponding sides from

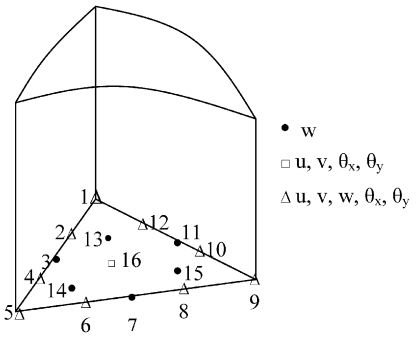

Fig. 1. A typical shell element projected in the base plane.

their nearest corner. The coordinates of the nodes 13, 14, 15 and 16 are (1/2, 1/4, 1/4), (1/4, 1/2, 1/4), (1/4, 1/4, 1/2) and (1/3, 1/3, 1/3), respectively. The degrees of freedom at nodes 1–12, (except 3, 7 and 11) are u, v, w, θ_x and θ_y. It is only w at nodes 3, 7, 11, 13, 14 and 15. The centroidal node has u, v, θ_x and θ_y as degrees of freedom.

The displacements (u, v and w) and rotations of the normal (θ_x and θ_y) have been taken as independent field variables and they may be expressed as

$$u = [P_1]\{\eta\}, \tag{1a}$$

$$v = [P_1]\{\beta\}, \tag{1b}$$

$$w = [P_2]\{\gamma\}, \tag{1c}$$

$$\theta_x = [P_1]\{\mu\} \tag{1d}$$

and

$$\theta_y = [P_1]\{\lambda\}, \tag{1e}$$

where

$$[P_1] = \begin{bmatrix} L_1^3 & L_2^3 & L_3^3 & L_1^2L_2 & L_2^2L_1 & L_2^2L_3 & L_3^2L_2 & L_3^2L_1 & L_1^2L_3 & L_1L_2L_3 \end{bmatrix},$$

$$[P_2] = [L_1^4 \quad L_2^4 \quad L_3^4 \quad L_1^3L_2 \quad L_2^3L_1 \quad L_2^3L_3 \quad L_3^3L_2 \quad L_3^3L_1 \quad L_1^3L_3 \quad L_1^2L_2^2 \quad L_2^2L_3^2 \quad L_3^2L_1^2 \quad L_1^2L_2L_3 \quad L_1L_2^2L_3 \quad L_1L_2L_3^2],$$

$$\{\eta\} = [\alpha_1 \quad \alpha_2 \quad \alpha_3 \quad \alpha_4 \quad \alpha_5 \quad \alpha_6 \quad \alpha_7 \quad \alpha_8 \quad \alpha_9 \quad \alpha_{10} \quad]^{\mathrm{T}}$$

$$\{\beta\} = [\alpha_{11} \quad \alpha_{12} \quad \alpha_{13} \quad \alpha_{14} \quad \alpha_{15} \quad \alpha_{16} \quad \alpha_{17} \quad \alpha_{18} \quad \alpha_{19} \quad \alpha_{20} \quad]^{\mathrm{T}}$$

$$\{\gamma\} = [\alpha_{21} \quad \alpha_{22} \quad \alpha_{23} \quad \alpha_{24} \quad \alpha_{25} \quad \alpha_{26} \quad \alpha_{27} \quad \alpha_{28} \quad \alpha_{29} \quad \alpha_{30} \quad \alpha_{31} \quad \alpha_{32} \quad \alpha_{33} \quad \alpha_{34} \quad \alpha_{35}]^{\mathrm{T}},$$

$$\{\mu\} = [\alpha_{36} \quad \alpha_{37} \quad \alpha_{38} \quad \alpha_{39} \quad \alpha_{40} \quad \alpha_{41} \quad \alpha_{42} \quad \alpha_{43} \quad \alpha_{44} \quad \alpha_{45}]^{\mathrm{T}}$$

and

$$\{\lambda\} = [\alpha_{46} \quad \alpha_{47} \quad \alpha_{48} \quad \alpha_{49} \quad \alpha_{50} \quad \alpha_{51} \quad \alpha_{52} \quad \alpha_{53} \quad \alpha_{54} \quad \alpha_{55}]^{\mathrm{T}}.$$

Now the above Eqs. (1a)–(1e) may be substituted appropriately at the different nodes of the element (Fig. 1) appropriately which will give the relationship between the unknown coefficients of the above polynomials (Eqs. (1)) and the nodal degrees of freedom as

$$\{\delta_e\} = [A]\{\alpha\} \text{ or } \{\alpha\} = [A]^{-1}\{\delta_e\}, \tag{2}$$

where

$$\{\alpha\} = [\alpha_1 \quad \alpha_2 - - - - - \alpha_{55}],$$

$$\{\delta_e\}^{\mathrm{T}} = [u_1 \quad v_1 \quad w_1 \quad \theta_{x1} \quad \theta_{y1} \quad u_2 \quad v_2 \quad w_2 \quad \theta_{x2} \quad \theta_{y2} \quad w_3 \quad u_4 \quad v_4 \quad w_4 \quad \theta_{x4} \quad \theta_{y4} \quad u_5 \quad v_5 \quad w_5 \quad \theta_{x5} \quad \theta_{y5} \quad u_6 \quad v_6 \quad w_6 \quad \theta_{x6} \quad \theta_{y6} \quad w_7 \quad u_8 \quad v_8 \quad w_8 \quad \theta_{x8} \quad \theta_{y8} \quad u_9 \quad v_9 \quad \theta_{x9} \quad \theta_{y9} \quad u_{10} \quad v_{10} \quad w_{10} \quad \theta_{x10} \quad \theta_{y10} \quad w_{11} \quad u_{12} \quad v_{12} \quad w_{12} \quad \theta_{x12} \quad \theta_{y12} \quad w_{13} \quad w_{14} \quad w_{15} \quad u_{16} \quad v_{16} \quad \theta_{x16} \quad \theta_{y16}]$$

and the matrix $[A]$ having an order of 55×55 contains the coordinates of the different nodes. As the rotations of the normal θ_x and θ_y are independent field variables and they are not derivatives of w, the effect of shear deformation can be easily incorporated as follows:

$$\begin{Bmatrix} \phi_x \\ \phi_y \end{Bmatrix} = \begin{Bmatrix} \theta_x - \partial w/\partial x \\ \theta_y - \partial w/\partial y \end{Bmatrix}, \tag{3}$$

where ϕ_x and ϕ_y are the average shear strain over the entire plate thickness and θ_x and θ_y are components of rotation of the normal.

The generalized stress strain relationship of a laminated plate may be written as

$$\{\sigma\} = [D]\{\varepsilon\}, \tag{4}$$

where

$$\{\sigma\}^{\mathrm{T}} = [N_x \quad N_y \quad N_{xy} \quad M_x \quad M_y \quad M_{xy} \quad Q_x \quad Q_y], \tag{5}$$

$$\{\varepsilon\} = \begin{Bmatrix} \partial u/\partial x + w/R_x \\ \partial v/\partial y \\ \partial u/\partial y + \partial v/\partial x \\ -\partial\theta_x/\partial x \\ -\partial\theta_y/\partial y \\ -\partial\theta_x/\partial y - \partial\theta_y/\partial x \\ \partial w/\partial x - \theta_x \\ \partial w/\partial y - \theta_y \end{Bmatrix} \tag{6}$$

and

$$[D] = \begin{bmatrix} A_{11} & A_{12} & A_{16} & B_{11} & B_{12} & B_{16} & 0 & 0 \\ A_{21} & A_{22} & A_{26} & B_{21} & B_{22} & B_{26} & 0 & 0 \\ A_{61} & A_{62} & A_{66} & B_{61} & B_{62} & B_{66} & 0 & 0 \\ B_{11} & B_{12} & B_{16} & D_{11} & D_{12} & D_{16} & 0 & 0 \\ B_{21} & B_{22} & B_{26} & D_{21} & D_{22} & D_{26} & 0 & 0 \\ B_{61} & B_{62} & B_{66} & D_{61} & D_{62} & D_{66} & 0 & 0 \\ 0 & 0 & 0 & 0 & 0 & 0 & A_{55} & A_{54} \\ 0 & 0 & 0 & 0 & 0 & 0 & A_{45} & A_{44} \end{bmatrix}. \tag{7}$$

The rigidity matrix $[D]$ constitutes of the contributions of its individual layers. Using the material properties and fiber orientation of the individual layers it can be easily obtained following the steps available in any standard text on mechanics of fiber reinforced laminated composites.

Now the field variables as expressed in Eqs. (1) may be substituted in Eq. (6) to express the strain vector $\{\varepsilon\}$ as

$$\{\varepsilon\} = [C]\{\alpha\}. \tag{8}$$

With the help of Eq. (2), the strain vector $\{\varepsilon\}$ in the above Eq. (8) may be expressed in terms of nodal displacement vector $\{\delta_e\}$ as

$$\{\varepsilon\} = [C][A]^{-1}\{\delta_e\} = [B]\{\delta_e\}. \tag{9}$$

Once the matrices, $[B]$ and $[D]$ are obtained, the element stiffness matrix $[K_e]$ can be easily derived using the virtual work technique and it may be expressed as

$$[K_e] = \int_A [B]^{\mathrm{T}}[D][B]\,\mathrm{d}x\,\mathrm{d}y. \tag{10}$$

In a similar manner, the consistent mass matrix of an element can be derived and it may be expressed with the help of Eqs. (1)–(2) as

$$[M_e] = \rho h \begin{pmatrix} \int_A [A^{-1}]^{\mathrm{T}}[Q_1]^{\mathrm{T}}[Q_1][A^{-1}]\,\mathrm{d}x\,\mathrm{d}y + \int_A [A^{-1}]^{\mathrm{T}}[Q_2]^{\mathrm{T}}[Q_2][A^{-1}]\,\mathrm{d}x\,\mathrm{d}y \\ + \int_A [A^{-1}]^{\mathrm{T}}[Q_3]^{\mathrm{T}}[Q_3][A^{-1}]\,\mathrm{d}x\,\mathrm{d}y + \dfrac{h^2}{12}\int_A [A]^{-\mathrm{T}}[Q_4]^{\mathrm{T}}[Q_4][A]^{-1}\partial x \partial y \\ + \dfrac{h^2}{12}\int_A [A]^{-\mathrm{T}}[Q_5]^{\mathrm{T}}[Q_5][A]^{-1}\partial x \partial y \end{pmatrix}, \tag{11}$$

where

$$\left[Q_1\right] = [P_1 \quad N_1 \quad N_2 \quad N_1 \quad N_1],\ \left[Q_2\right] = [N_1 \quad P_1 \quad N_2 \quad N_1 \quad N_1],$$

$$\left[Q_3\right] = [N_1 \quad N_1 \quad P_2 \quad N_1 \quad N_1],\ \left[Q_4\right] = [N_1 \quad N_1 \quad N_2 \quad P_1 \quad N_1]$$

and

$$\left[Q_5\right] = [N_1 \quad N_1 \quad N_2 \quad N_1 \quad P_1].$$

In the above equations $[N_1]$ and $[N_2]$ are null matrices of order 1×10 and 1×15, respectively. The first two terms of the mass matrix in Eq. (11) is associated with in-plane movements of mass, third term indicates transverse move of mass (which is usually found to contribute the major inertia) while the last two terms are associated with rotary inertia and their contribution becomes significant only in a shell having higher thickness ratio.

Though the consistent mass matrix presented in Eq. (11) indicates all the contributions including rotary inertia it cannot be used. With this mass matrix the degrees of freedom at internal nodes (which contains sufficient amount of mass) cannot be eliminated but it is desired to eliminate these quantities for the improvement of computational elegance. The above problem has been avoided by using a lumped mass matrix where the mass of an element is to be distributed at the external nodes only. In this context two different mass lumping schemes have been recommended, which are as follows.

In the first lumping scheme, the mass of an element m_e has been taken at the degrees of freedom w of all the external nodes. Thus the mass matrix contains twelve non-zero elements at twelve diagonals and their summation is equal to the mass of the element. The distribution of mass of an element at these twelve degrees of freedom has been made in proportion to the diagonal elements of the consistent mass matrix (Eq. (11)). The idea is similar to that of Hinton et al. [12] except that the mass at some of the nodes has not been taken in the present case. This mass lumping scheme has been defined as LS12 and it is as follows:

$$m_{ii}^{wl} = \frac{m_{ii}}{\sum m_{ii}} m_e (I = 3,\ 8,\ 11,\ 14,\ 19,\ 24,\ 27,\ 30,\ 35,\ 40,\ 43,\ 46),$$

where m_{ii}^{wl} are the ith diagonal elements corresponding to w of the proposed lumped mass matrix and m_{ii} is the ith diagonal element of the consistent mass matrix $[M_e]$.

In the second lumping scheme (LS9RI), the effect of rotary inertia (as well as in-plane effect) has been taken into account, which will be mass contributions in addition to those (m_{ii}^{wl}) taken in the previous case (LS12). In this lumping scheme the external nine nodes containing the degrees of freedom of u, v, w, θ_x and θ_y have been considered. Similar technique has been followed to get it at the external nodes as follows:

$$m_{ii}^{ul} = \frac{m_{ii}}{\sum m_{ii}} m_e \quad (i = 1,\ 6,\ 12,\ 17,\ 22,\ 28,\ 33,\ 38,\ 44),$$

$$m_{ii}^{vl} = \frac{m_{ii}}{\sum m_{ii}} m_e \quad (i = 2,\ 7,\ 13,\ 18,\ 23,\ 29,\ 34,\ 39,\ 45),$$

$$m_{ii}^{wl} = \frac{m_{ii}}{\sum m_{ii}} m_e \quad (i = 3,\ 8,\ 11,\ 14,\ 19,\ 24,\ 27,\ 30,\ 35,\ 40,\ 43,\ 46),$$

$$m_{ii}^{\theta xl} = \frac{h^2}{12}\frac{m_{ii}}{\sum m_{ii}} m_e \quad (i = 4,\ 9,\ 15,\ 20,\ 25,\ 31,\ 36,\ 41,\ 47)$$

and

$$m_{ii}^{\theta yl} = \frac{h^2}{12}\frac{m_{ii}}{\sum m_{ii}} m_e \quad (I = 3,\ 8,\ 11,\ 14,\ 19,\ 24,\ 27,\ 30,\ 35,\ 40,\ 43,\ 46),$$

where the use of $(h^2/12)$ can be justified with the expression of the consistent mass matrix as presented in Eq. (11)

Following any one of the above two lumping schemes, the mass matrix can be formed, which will be diagonal matrix having zero mass at the degrees of freedom of the internal nodes. With such a mass matrix, it is easy to perform the static condensation of the internal nodes of the element.

In this stage, the order of $[K_e]$ and $\{M_e\}$ is fifty-five, which is reduced to forty-eight by eliminating the degrees of freedom of the internal nodes (w_{13}, w_{14}, w_{15}, u_{16}, v_{16}, θ_{x16} and θ_{y16}) through static condensation.

The stiffness matrix and mass matrix having an order of forty eight in their final form has been evaluated for all the elements and they have been assembled together to form the overall stiffness $[K]$ and mass matrix $[M]$, respectively. Once $[K]$ and $[M]$ are obtained, the equation of motion of the plate may be expressed as

$$[K] = \omega^2[M]. \tag{12}$$

After incorporating the boundary conditions in the above equation it has been solved by simultaneous iterative technique [13] to get frequency ω for first few modes.

3. Results and discussions

Numerical example of composite skewed cylindrical shell panels are solved by the proposed composite shallow shell element. Isotropic skewed cylindrical shell panels and a laminated composite shell panels are solved and compared with the published results to validate the present finite element formulation.

3.1. Isotropic skewed cylindrical shell and composite shell panels

An isotropic open cylindrical shell fixed along the curved edges (Figs. 2 and 3) and other two straight edges free is analyzed for three different values of thickness to radius ratio h/R (0.01, 0.1 and 0.2). The analysis is

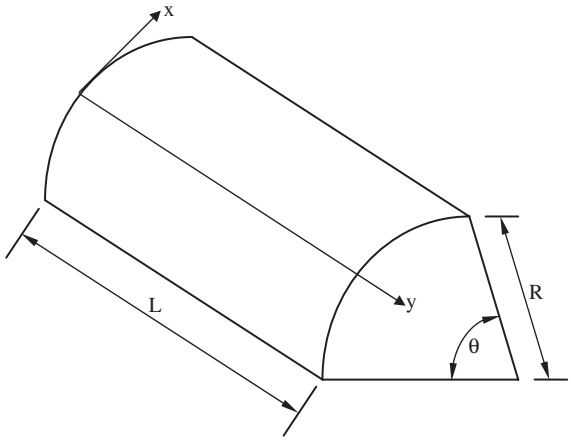

Fig. 2. Cylindrical shell panel with dimensions.

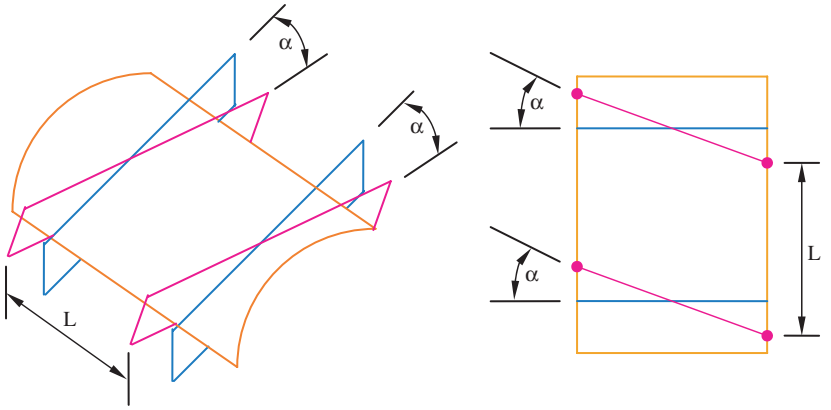

Fig. 3. Three dimensional and top view of skewed cylindrical shell panels.

Table 1
Comparison of the first five frequency parameter $\lambda = \omega R\sqrt{\rho/E}$ for isotropic skew cylindrical shell panel fixed at the curved edges with $\alpha = 45^\circ$, $\theta = 60^\circ$ and $L/R = 4.0$

h/R	Source	Mode number				
		1	2	3	4	5
0.01	LS12 (8 × 3)[a]	0.024	0.040	0.059	0.062	0.088
	LS12 (10 × 4)	0.024	0.040	0.059	0.061	0.086
	LS12 (13 × 5)	0.024	0.040	0.059	0.061	0.085
	LS9RI (8 × 3)	0.025	0.041	0.052	0.065	0.089
	LS9RI (10 × 4)	0.024	0.040	0.060	0.063	0.088
	LS9RI (13 × 5)	0.024	0.040	0.059	0.062	0.087
	Kandasamy and Singh [11]	0.024	0.040	0.059	0.062	0.084
0.1	LS12 (8 × 3)	0.078	0.117	0.212	0.240	0.374
	LS12 (10 × 4)	0.087	0.117	0.212	0.240	0.375
	LS12 (13 × 5)	0.087	0.117	0.212	0.240	0.375
	LS9RI (8 × 3)	0.084	0.117	0.203	0.239	0.363
	LS9RI (10 × 4)	0.084	0.116	0.203	0.237	0.362
	LS9RI (13 × 5)	0.084	0.115	0.202	0.236	0.361
0.2	LS12 (8 × 3)	0.127	0.208	0.335	0.413	0.626
	LS12 (10 × 4)	0.127	0.208	0.334	0.414	0.628
	LS12 (13 × 5)	0.127	0.208	0.334	0.415	0.629
	LS9RI (8 × 3)	0.122	0.204	0.316	0.389	0.403
	LS9RI (10 × 4)	0.121	0.202	0.315	0.388	0.401
	LS9RI (13 × 5)	0.121	0.202	0.315	0.388	0.400

[a]Present analysis based on mesh division 8 × 3 using the mass lumping scheme LS12, which is similarly applicable for other mesh divisions and mass lumping scheme.

performed considering skew angle $\alpha = 45^\circ$, subtended angle $\theta = 60^\circ$ and $L/R = 4.0$. The first five natural frequencies obtained with both the mass lumping schemes (LS12 and LS9RI) are presented in Table 1 for different mesh division with those of Kandasamy and Singh [11]. For $h/R = 0.01$ the present results are very close to the solution of Kandasamy and Singh [11]. Kandasamy and Singh [11] analyzed the problem using Rayleigh–Ritz method.

A cantilever square symmetric cross ply (0/90/0) shell panel (cylindrical, spherical and saddle type) having thickness ratio $h/a = 0.01$ is analyzed using both the mass lumping schemes (LS12 and LS9RI). The first five

Table 2
First five frequency parameter $\lambda = (\omega a^2\sqrt{\rho/E_1})/h$ for cantilever composite (0/90/0) square shell panel fixed at one curved edge with, $E_1 = 138.0\,\text{GPa}$, $E_2 = 8.96\,\text{GPa}$, $G_{12} = 7.1\,\text{GPa}$, $\nu_{12} = 0.3$, $h/a = 0.01$and $a/R = 0.5$

Shell type	Sources	Mode number				
		1	2	3	4	5
Saddle $R_y/R_x = -1.0$	LS12 (6×6)	1.4875	1.5759	5.9754	7.1698	11.388
	LS12 (8×8)	1.4929	1.5779	6.0322	7.2178	11.517
	LS12 (10×10)	1.4981	1.5823	6.0606	7.2465	11.574
	LS9RI (6×6)	1.4495	1.5434	5.8940	6.7969	11.002
	LS9RI (8×8)	1.4579	1.5476	5.9560	6.8451	11.166
	LS9RI (10×10)	1.4630	1.5502	5.9833	6.8749	11.237
	Chakraborty et al. [14]	1.4643				
Cylindrical	LS12 (6×6)	1.8542	2.4407	4.5910	6.3239	7.8281
	LS12 (8×8)	1.8625	2.4482	4.6023	6.3581	7.9762
	LS12 (10×10)	1.8644	2.4512	4.6066	6.3744	8.0486
	LS9RI (6×6)	1.8564	2.4632	4.5530	6.4833	7.7880
	LS9RI (8×8)	1.8638	2.4594	4.5588	6.4435	7.9454
	LS9RI (10×10)	1.8647	2.4541	4.5599	6.4243	8.0232
	Chakraborty et al. [14]	1.8649				
Spherical $R_y/R_x = 1.0$	LS12 (6×6)	1.5540	1.9399	4.9618	6.9401	8.4938
	LS12 (8×8)	1.5587	1.9465	5.0073	7.0205	8.5955
	LS12 (10×10)	1.5622	1.9515	5.0302	7.0591	8.6425
	LS9RI (6×6)	1.5248	1.8895	4.9247	6.5370	8.2449
	LS9RI (8×8)	1.5297	1.9012	4.9632	6.6148	8.3616
	LS9RI (10×0)	1.5323	1.9068	4.9819	6.6519	8.4142
	Chakraborty et al. [14]	1.5361				

natural frequencies obtained are presented in Table 2 with those of Chakraborty et al. [14]. The present results obtained by mass lumping scheme LS9RI are very close to the solutions of Chakraborty et al. [14].

From Tables 1 and 2, it is seen that for thin isotropic shell both the proposed mass lumping schemes are equally good. As thickness to radius ratio increases effect of rotary inertia also increases. Therefore, for thin isotropic shells both the mass lumping schemes are recommended whereas for thick isotropic shells and composite shells of any thickness mass lumping scheme LS9RI is recommended.

Both the above examples are given for validation of the present element, formulation and proposed mass lumping schemes.

3.2. Laminated composite skewed cylindrical shell panels

Laminated composite skewed cylindrical shell panel fixed along one curved edges (Figs. 2 and 3) and other three edges free is analyzed for $h/R = 0.01$. The analysis is performed considering skew angle $\alpha = 45^\circ$, subtended angle $\theta = 60^\circ$ and $L/R = 4.0$. Both symmetric and anti-symmetric cross ply having different layer numbers are investigated. The first five natural frequencies obtained by the mass lumping scheme LS9RI are presented in Table 3 for different mesh division. From Table 3 it is seen that for same thickness ratio as number of layer increases frequencies also increase for anti-symmetric ply and it is reverse for symmetric ply.

Four layer anti-symmetric angle ply skewed composite cylindrical shell panel fixed along one curved edge and other three edges free having different fiber orientations is analyzed. Effect of different L/R ratios (1, 2 and 4) and fiber orientation angles is investigated in this example. The analysis is performed considering skew angle $\alpha = 45^\circ$, $h/R = 0.1$ and subtended angle $\theta = 30^\circ$. The first five natural frequencies obtained using mass lumping scheme LS9RI is presented in Table 4 considering mesh divisions 20×3. From Table 4 it is seen that frequency is maximum for lamination scheme $15/-15/15/-15$ in all the cases.

Table 3
First five frequency parameter $\lambda = (\omega R\sqrt{\rho/E})/h$ for cantilever skew composite cylindrical shell panel fixed at one curved edge with $\alpha = 45^\circ$, $\theta = 60^\circ$, $h/R = 0.01$ and $L/R = 4.0$, $E_1/E_2 = 40$, $G_{23} = 0.5E_2$, $G_{13} = G_{13} = 0.6E_2$ and $v_{12} = 0.25$

Lamination schemes (deg.)	Source	Mode number				
		1	2	3	4	5
For anti-symmetric lamination						
0/90	LS9RI (10 × 4)	1.442	3.428	6.366	9.506	12.944
	LS9RI (13 × 5)	1.436	3.426	6.387	9.525	12.985
	LS9RI (16 × 6)	1.433	3.426	6.404	9.566	12.995
0/90/0/90	LS9RI (10 × 4)	1.478	3.508	6.704	10.694	14.952
	LS9RI (13 × 5)	1.473	3.508	6.726	10.753	15.024
	LS9RI (16 × 6)	1.470	3.508	6.741	10.813	15.126
0/90/0/90/0	LS9RI (10 × 4)	1.484	3.523	6.770	10.908	15.242
90/0/90/0/90	LS9RI (13 × 5)	1.481	3.522	6.791	10.970	15.329
	LS9RI (16 × 6)	1.479	3.522	6.806	11.031	15.435
For symmetric lamination						
0/90/0	LS9RI (10 × 4)	1.595	3.737	6.837	8.900	9.975
	LS9RI (13 × 5)	1.590	3.734	6.853	8.809	9.809
	LS9RI (16 × 6)	1.588	3.734	6.869	8.775	9.734
0/90/0/90/0	LS9RI (10 × 4)	1.568	3.730	7.020	10.833	14.936
	LS9RI (13 × 5)	1.563	3.731	7.043	10.862	14.989
	LS9RI (16 × 6)	1.560	3.731	7.059	10.894	14.999
0/90/0/90/0/90/0	LS9RI (10 × 4)	1.539	3.653	6.942	10.942	15.200
	LS9RI (13 × 5)	1.534	3.654	6.964	10.988	15.257
	LS9RI (16 × 6)	1.532	3.654	6.980	11.032	15.310

Table 4
First five frequency parameter $\lambda = (\omega R\sqrt{\rho/E})/h$ for cantilever skew composite cylindrical shell panel fixed at one curved edge with $\theta = 30^\circ$, $h/R = 0.1$ and $\alpha = 45^\circ$. $E_1/E_2 = 40$, $G_{23} = 0.5E_2$, $G_{13} = G_{13} = 0.6E_2$ and $v_{12} = 0.25$

L/R	Lamination scheme (deg.)	Mode number				
		1	2	3	4	5
4	15/−15/15/−15	0.355	1.741	1.968	2.348	5.304
	30/−30/30/−30	0.214	0.990	1.303	3.008	3.597
	45/−45/45/−45	0.119	0.550	0.737	2.046	3.240
	60/−60/60/−60	0.084	0.408	0.521	1.431	2.452
2	15/−15/15/−15	1.448	4.446	6.460	7.960	12.810
	30/−30/30/−30	0.966	4.077	4.955	6.812	12.444
	45/−45/45/−45	0.561	2.373	3.226	6.902	8.442
	60/−60/60/−60	0.384	1.768	2.258	5.679	6.597
1	15/−15/15/−15	5.583	11.981	19.574	22.676	23.865
	30/−30/30/−30	4.314	11.687	15.155	20.024	23.221
	45/−45/45/−45	2.782	9.606	11.432	16.711	21.868
	60/−60/60/−60	1.876	7.411	8.956	14.910	17.473

The effect of skew angle (α) on free vibration of four layer symmetric cross ply (0/90/90/0) skewed cylindrical shell panel fixed at one curved edge and other three edges free is investigated in this example. Shells having $h/R = 0.01$, 0.1 and 0.2 and $\theta = 60^o$ and 30^o are analyzed. The first five natural frequencies obtained are presented in Table 5 considering mesh divisions 16×3 for $\theta = 30^o$ and 20×5 for $\theta = 60^o$. It is seen that as skew angle increases natural frequencies also increase.

Table 5
First five frequency parameter $\lambda = (\omega R\sqrt{\rho/E})/h$ for cantilever skew composite (0/90/90/0) cylindrical shell panel fixed at one curved edge with $L/R = 4.0$. $E_1/E_2 = 40$, $G_{23} = 0.5E_2$, $G_{13} = G_{13} = 0.6E_2$ and $\nu_{12} = 0.25$

θ (deg.)	Skew angle (α) (deg.)	h/R	Mode number				
			1	2	3	4	5
60	15	0.01	1.399	3.438	6.390	11.404	14.047
	30		1.412	3.402	6.462	10.892	13.950
	45		1.482	3.479	6.723	10.097	13.494
	15	0.1	0.501	0.784	2.103	2.628	2.920
	30		0.503	0.796	2.137	2.651	2.943
	45		0.521	0.814	2.210	2.723	3.009
	15	0.2	0.389	0.708	1.054	1.978	2.444
	30		0.397	0.716	1.077	2.000	2.459
	45		0.402	0.727	1.135	2.062	2.478
30	15	0.01	1.042	1.461	5.008	5.779	10.289
	30		1.045	1.475	5.045	5.795	10.389
	45		1.057	1.491	5.048	5.840	10.436
	15	0.1	0.381	1.256	1.343	2.253	4.094
	30		0.383	1.259	1.356	2.269	4.090
	45		0.387	1.259	1.383	2.306	4.067
	15	0.2	0.362	0.670	1.047	1.904	2.836
	30		0.363	0.676	1.053	1.917	2.894
	45		0.367	0.689	1.061	1.947	2.979

Table 6
First five frequency parameter $\lambda = (\omega R\sqrt{\rho/E})/h$ for cantilever skew composite cylindrical shell panel fixed at one curved edge with $L/R = 4.0$, $\theta = 30^\circ$, $h/R = 0.1$ $E_1/E_2 = 40$, $G_{23} = 0.5E_2$, $G_{13} = G_{13} = 0.6E_2$ and $\nu_{12} = 0.25$

Skew angle (α) (deg.)	Lamination scheme (deg.)	Mode number				
		1	2	3	4	5
15	0/90	0.188	1.098	1.159	1.366	2.979
	0/60	0.192	1.148	1.290	1.477	3.082
	0/45	0.202	1.205	1.375	1.658	3.242
	0/30	0.225	1.313	1.431	1.853	3.552
	0/15	0.293	1.402	1.555	2.025	4.061
30	0/90	0.190	1.078	1.194	1.386	2.949
	0/60	0.196	1.150	1.315	1.509	3.087
	0/45	0.207	1.212	1.399	1.700	3.251
	0/30	0.231	1.313	1.462	1.907	3.536
	0/15	0.300	1.391	1.578	2.101	3.980
45	0/90	0.195	1.064	1.239	1.427	2.919
	0/60	0.203	1.157	1.354	1.564	3.101
	0/45	0.215	1.225	1.440	1.765	2.264
	0/30	0.240	1.316	1.510	1.985	3.514
	0/15	0.311	1.374	1.615	2.199	3.892

Same cylindrical shell panel having various fiber orientation angles is analyzed considering $h/R = 0.1$, $L/R = 4.0$ and $\theta = 30^\circ$. The analysis is performed considering skew angle $\alpha = 15^\circ$, 30° and 45°. The first five natural frequencies obtained using mass lumping scheme LS9RI is presented in Table 6 considering mesh divisions 16×3. From Table 6 it is seen that frequency is maximum for lamination scheme 0/15 in all the cases.

4. Conclusions

A triangular composite shallow shell element is used for free vibration of composite skewed cylindrical shell panels. The effect of shear deformation is incorporated in the element formulation in such a way that there is no shear locking problem. As there is no suitable results for free vibration of composite skewed shell panels, the present formulation is tested with published isotropic skewed cylindrical shell panel and composite shell panel. The first two examples show that the present element formulation is very effective for both isotropic and composite shell panels. The proposed mass lumped schemes are very efficient and one of them is recommended for free vibration of both thick and thin shells. Analysis is performed for free vibration of composite skewed cylindrical shell panels having different length to radius ratios, skew angles, thickness to radius ratios, fiber orientation angles and number of layers. It is expected that these new results for free vibration of skewed composite cylindrical shell panels will be useful in future research.

References

[1] J.L. Sanders, An improved first approximation theory of thin shells. NASA Report 24, 1959.
[2] W. Flugge, *Stresses in Shells*, Springer, New York, 1960.
[3] F.I. Niordson, A consistant refined shell theory. In: Complete Analysis and its Applications, Vekua Anniveesary Volume, Nauka, Moscow, 1978, pp. 421–429.
[4] M.S. Qatu, Recent research advances in the dynamic behavior of shells, *Applied Mechanics Reviews* 55 (Part I) (2002) 325–350.
[5] M.S. Qatu, Recent research advances in the dynamic behavior of shells, *Applied Mechanics Reviews* 55 (Part II) (2002) 415–434.
[6] A. Selmane, A.A. Lakis, Dynamic analysis of anisotropic open cylindrical shells, *Computers and Structures* 62 (1997) 1–12.
[7] S.J. Lee, S.E. Han, Free vibration analysis of plates and shells with a nine-node assumed natural degenerated shell element, *Journal of Sound and Vibration* 241 (4) (2001) 605–633.
[8] L. Liu, L.P. Chua, D.N. Ghista, Element free Galerkin method for static and dynamic analysis of spatial shell structures, *Journal of Sound and Vibration* 295 (2006) 388–406.
[9] G.V. Voyiadjis, P. Woelke, A refined theory for thick spherical shells, *Solids and Structures* 41 (2004) 3747–3769.
[10] S.J. Hossain, P.K. Sinha, A.H. Sheikh, A finite element formulation for the analysis of laminated composite shells, *Computer and Structures* 82 (2004) 1623–1638.
[11] S. Kandasamy, A.V. Shing, Free vibration analysis of skewed open circular cylindrical shells, *Journal of Sound and Vibration* 290 (2006) 1100–1118.
[12] E. Hintal, T. Rock, O.C. Zienkiewicz, A note on mass lumping and related processes in the finite element method, *Earthquake Engineering and Structural Dynamics* 4 (1976) 245–249.
[13] R.B. Corr, A. Jennings, A simultaneous iteration algorithm for symmetric eigenvalue problems, *International Journal of Numerical Methods and Engineering* 18 (1951) 31–38.
[14] D. Chakraborty, P.K. Sinha, J.N. Bandyopadhyay, Application of FEM on free and forced vibration of laminated shells, *Journal of Engineering Mechanics, ASCE* 124 (1) (1998) 1–8.